

Phenomenology of Two-Texture Zero Neutrino Mass Matrices

S. Dev*, Sanjeev Kumar†, Surender Verma‡ and Shivani Gupta§

Department of Physics, Himachal Pradesh University, Shimla 171005,
INDIA

Abstract

The generic predictions of two-texture zero neutrino mass matrices in the flavor basis have been examined especially in relation to the degeneracies between mass matrices within a class and interesting constraints on the neutrino parameters have been obtained. It is shown that the deviation of the atmospheric mixing angle from maximality and the quadrant of the Dirac-type CP-violating phase δ can be used to lift these degeneracies.

1 Introduction

Mass matrices provide important tools for the investigation of the underlying symmetries and the resulting dynamics. The first step in this direction is the reconstruction of the neutrino mass matrix in the flavor basis. However, the reconstruction results in a large variety of possible structures of mass matrices depending strongly on the mass scale, mass hierarchy and the Majorana phases. However, the relatively weak dependence on some oscillation parameters (θ_{23} and δ) results in the degeneracy of possible neutrino mass matrices. The mass matrix for Majorana neutrinos contains nine physical parameters including the three mass eigenvalues, three mixing angles and the three CP-violating phases. The two squared-mass differences (Δm_{21}^2 and Δm_{32}^2) and the two mixing angles (θ_{12} and θ_{23}) have been measured in solar, atmospheric and reactor experiments. The third mixing angle θ_{13} and the Dirac-type CP-violating phase δ are expected to be measured in the forthcoming neutrino oscillation experiments. The possible measurement of the effective Majorana mass in neutrinoless double β decay searches will provide an additional constraint on the remaining three neutrino

*dev5703@yahoo.com

†sanjeev3kumar@gmail.com

‡s_7verma@yahoo.co.in

§shiroberts_1980@yahoo.co.in

parameters viz. the neutrino mass scale and two Majorana-type CP-violating phases. While the neutrino mass scale will, independently, be determined by the direct beta decay searches and cosmological observations, it will not be possible to deduce the two Majorana phases uniquely determined from the measurement of effective Majorana mass even if the absolute neutrino mass scale is known. Under the circumstances, it is natural to employ other theoretical inputs for the reconstruction of the neutrino mass matrix. The form of these additional theoretical inputs are limited by the existing neutrino data. Several proposals have been made in the literature to restrict the form of the neutrino mass matrix and to reduce the number of free parameters which include presence of texture zeros [1, 2, 3, 4, 5], requirement of zero determinant [6], the zero trace condition [7] to name a few. However, the current neutrino oscillation data are consistent only with a limited number of texture schemes [1, 2, 3, 4, 5]. In particular, the current neutrino oscillation data disallow all neutrino mass matrices with three or more texture zeros in the flavor basis. Out of the fifteen possible neutrino mass matrices with two texture zeros, only seven are compatible with the current neutrino oscillation data. The seven allowed two texture zero mass matrices have been classified into three categories. The two class A matrices of the types A_1 and A_2 give normal hierarchy (NH) of neutrino masses. The class B matrices of types B_1 , B_2 , B_3 and B_4 yield a quasi-degenerate (QD) spectrum of neutrino masses. The single class C matrix corresponds to inverted hierarchy (IH) of neutrino masses.

In the present work, we examine phenomenological implications of all possible neutrino mass matrices with two texture zeros. Neutrino mass matrices within a class were thought to have identical phenomenological consequences [1, 2, 3] leading to degeneracy of mass matrices within a class. Thus, there is a two-fold degeneracy in class A while the neutrino mass matrices of class B exhibit an eight-fold degeneracy since Normal/Inverted hierarchies are practically indistinguishable because of quasi-degenerate spectrum of neutrino masses in this class. We study this degeneracy in details and discuss the possible ways to lift this degeneracy. It is found that the deviation of atmospheric mixing from maximality and the quadrant of the Dirac-type CP-violating phase δ can be used to distinguish the mass matrices within a class. We, also, note that the determination of hierarchy will have important implications for class B neutrino mass matrices. The prospects for the measurement of θ_{13} for class A neutrino mass matrices are quite optimistic since a definite lower bound on θ_{13} is obtained for this class. For neutrino mass matrices of class B, CP-violation will be near maximal if θ_{13} is large. Definite lower bounds on the effective Majorana mass M_{ee} are obtained for neutrino mass matrices of class B and C. Class D of neutrino mass matrices is disallowed in our analysis.

2 Neutrino mass matrix

The neutrino mass matrix, M , can be parameterized in terms of three neutrino mass eigenvalues (m_1 , m_2 , m_3), three neutrino mixing angles (θ_{12} , θ_{23} , θ_{13}) and one Dirac-type CP violating phase, δ . If neutrinos are Majorana particles then there are two additional CP violating phases α , β in the neutrino mixing matrix. The complex symmetric mass matrix

M can be diagonalized by a complex unitary matrix V :

$$M = V M_\nu^{diag} V^T \quad (1)$$

where $M_\nu^{diag} = \text{Diag}\{m_1, m_2, m_3\}$. The neutrino mixing matrix V [8] can be written as

$$V \equiv UP = \begin{pmatrix} c_{12}c_{13} & s_{12}c_{13} & s_{13}e^{-i\delta} \\ -s_{12}c_{23} - c_{12}s_{23}s_{13}e^{i\delta} & c_{12}c_{23} - s_{12}s_{23}s_{13}e^{i\delta} & s_{23}c_{13} \\ s_{12}s_{23} - c_{12}c_{23}s_{13}e^{i\delta} & -c_{12}s_{23} - s_{12}c_{23}s_{13}e^{i\delta} & c_{23}c_{13} \end{pmatrix} \begin{pmatrix} 1 & 0 & 0 \\ 0 & e^{i\alpha} & 0 \\ 0 & 0 & e^{i(\beta+\delta)} \end{pmatrix}, \quad (2)$$

where $s_{ij} = \sin \theta_{ij}$ and $c_{ij} = \cos \theta_{ij}$. The matrix V is called the neutrino mixing matrix or PMNS matrix. The matrix U is the lepton analogue of the CKM quark mixing matrix and P contains the two Majorana phases.

The elements of the mass matrix neutrino mass matrix can be calculated from Eq. (1). Some of the elements of M , which can be equated to zero in the various allowed texture zero schemes, are given by

$$M_{ee} = c_{13}^2 c_{12}^2 m_1 + c_{13}^2 s_{12}^2 m_2 e^{2i\alpha} + s_{13}^2 m_3 e^{2i\beta}, \quad (3)$$

$$M_{e\mu} = c_{13}\{s_{13}s_{23}e^{i\delta}(e^{2i\beta}m_3 - s_{12}^2e^{2i\alpha}m_2) - c_{12}c_{23}s_{12}(m_1 - e^{2i\alpha}m_2) - c_{12}^2s_{13}s_{23}e^{i\delta}m_1\}, \quad (4)$$

$$M_{e\tau} = c_{13}\{s_{13}c_{23}e^{i\delta}(e^{2i\beta}m_3 - s_{12}^2e^{2i\alpha}m_2) + c_{12}s_{23}s_{12}(m_1 - e^{2i\alpha}m_2) - c_{12}^2s_{13}c_{23}e^{i\delta}m_1\}. \quad (5)$$

$$M_{\mu\mu} = m_1(c_{23}s_{12} + e^{i\delta}c_{12}s_{13}s_{23})^2 + e^{2i\alpha}m_2(c_{12}c_{23} - e^{i\delta}s_{12}s_{13}s_{23})^2 + e^{2i(\beta+\delta)}m_3c_{13}^2s_{23}^2 \quad (6)$$

and

$$M_{\tau\tau} = m_1(s_{23}s_{12} - e^{i\delta}c_{12}s_{13}c_{23})^2 + e^{2i\alpha}m_2(c_{12}s_{23} + e^{i\delta}s_{12}s_{13}c_{23})^2 + e^{2i(\beta+\delta)}m_3c_{13}^2c_{23}^2. \quad (7)$$

It will be helpful to note from Eqs. (4-7) that the transformation

$$T \quad : \quad \theta_{23} \rightarrow \frac{\pi}{2} - \theta_{23}, \delta \rightarrow \delta + \pi \quad (8)$$

transforms $M_{e\mu}$ to $-M_{e\tau}$ and $M_{\mu\mu}$ to $M_{\tau\tau}$. Therefore, if $M_{e\mu}$ vanishes for θ_{23} and δ , then $M_{e\tau}$ vanishes for $\frac{\pi}{2} - \theta_{23}$ and $\delta + \pi$. Similarly, if $M_{\mu\mu}$ vanishes for θ_{23} and δ , then $M_{\tau\tau}$ vanishes for $\frac{\pi}{2} - \theta_{23}$ and $\delta + \pi$. This fact can be, gainfully, used in distinguishing the subcategories of neutrino neutrino mass matrices within a class.

3 Two texture zeros

The neutrino mass matrix, M , in the charged lepton basis is given by Eq. (1). Out of the fifteen possible patterns for two texture zeros in M , the seven possibilities [1, 2], which are found to be in accordance with the current neutrino oscillation data, are listed in Table 1. In addition, we have, also, included the two mass matrices of class D in the list. These mass matrices were found to be disallowed in earlier analyses [1, 2]. However, it was found in a subsequent detailed numerical analysis by Guo and Xing [3] that the neutrino mass matrices

Type	Constraining Eqs.
A_1	$M_{ee} = 0, M_{e\mu} = 0$
A_2	$M_{ee} = 0, M_{e\tau} = 0$
B_1	$M_{e\tau} = 0, M_{\mu\mu} = 0$
B_2	$M_{e\mu} = 0, M_{\tau\tau} = 0$
B_3	$M_{e\mu} = 0, M_{\mu\mu} = 0$
B_4	$M_{e\tau} = 0, M_{\tau\tau} = 0$
C	$M_{\mu\mu} = 0, M_{\tau\tau} = 0$
D_1	$M_{\mu\mu} = 0, M_{\mu\tau} = 0$
D_2	$M_{\tau\tau} = 0, M_{\mu\tau} = 0$

Table 1: Allowed two texture zero mass matrices.

of class D are marginally allowed. The expressions for the vanishing elements in different two-zero texture schemes have been listed in Eqs. (4-7).

The transformation T defined in Eq. (8) transforms neutrino mass matrices of type A_1 to A_2 and neutrino mass matrices of type B_1 (B_4) to B_2 (B_3). Therefore, the predictions of neutrino mass matrices for types A_1 and A_2 will be identical for all neutrino parameters except θ_{23} and δ . Similarly, the predictions of neutrino mass matrices for all the four types of mass matrices in class B will be identical for all neutrino parameters except θ_{23} and/or δ .

The two texture zeroes in the neutrino mass matrix give two complex equations viz.

$$M_{ab} = 0, M_{pq} = 0 \quad (9)$$

where a, b, p and q can take values e, μ and τ . Eqs. (9) can, also, be written as

$$m_1 U_{a1} U_{b1} + m_2 U_{a2} U_{b2} e^{2i\alpha} + m_3 U_{a3} U_{b3} e^{2i(\beta+\delta)} = 0 \quad (10)$$

and

$$m_1 U_{p1} U_{q1} + m_2 U_{p2} U_{q2} e^{2i\alpha} + m_3 U_{p3} U_{q3} e^{2i(\beta+\delta)} = 0 \quad (11)$$

where U has been defined in Eq. (2). These two complex equations involve nine physical parameters $m_1, m_2, m_3, \theta_{12}, \theta_{23}, \theta_{13}$ and CP-violating phases α, β , and δ . The two mixing angles (θ_{12}, θ_{23}) and two mass-squared differences ($\Delta m_{12}^2, \Delta m_{23}^2$) are known from the solar, atmospheric and reactor neutrino experiments. The masses m_2 and m_3 can be calculated from the mass-squared differences Δm_{12}^2 and Δm_{23}^2 using the relations

$$m_2 = \sqrt{m_1^2 + \Delta m_{12}^2} \quad (12)$$

and

$$m_3 = \sqrt{m_2^2 + \Delta m_{23}^2}. \quad (13)$$

Thus, we have two complex relations relating five unknown parameters viz. $m_1, \theta_{13}, \alpha, \beta$ and δ . Therefore, if one out of these five parameters is assumed, other four parameters can be predicted. Thus, neutrino mass matrices with two texture zeros in the flavor basis have strong predictive power.

On solving Eqs. (10) and (11) simultaneously, we obtain

$$\frac{m_1}{m_3} e^{-2i\beta} = \frac{U_{p3}U_{q3}U_{a2}U_{b2} - U_{a3}U_{b3}U_{p2}U_{q2}}{U_{a1}U_{b1}U_{p2}U_{q2} - U_{a2}U_{b2}U_{p1}U_{q1}} \times e^{2i\delta}, \quad (14)$$

and

$$\frac{m_1}{m_2} e^{-2i\alpha} = \frac{U_{p2}U_{q2}U_{a3}U_{b3} - U_{a2}U_{b2}U_{p3}U_{q3}}{U_{a1}U_{b1}U_{p3}U_{q3} - U_{a3}U_{b3}U_{p1}U_{q1}}. \quad (15)$$

Using Eqs. (15) and (16), the two mass ratios $\left(\frac{m_1}{m_2}, \frac{m_1}{m_2}\right)$ and Majorana phases (α, β) can be written as

$$\left(\frac{m_1}{m_2}\right) = \left| \frac{U_{p2}U_{q2}U_{a3}U_{b3} - U_{a2}U_{b2}U_{p3}U_{q3}}{U_{a1}U_{b1}U_{p3}U_{q3} - U_{a3}U_{b3}U_{p1}U_{q1}} \right|, \quad (16)$$

$$\left(\frac{m_1}{m_3}\right) = \left| \frac{U_{p3}U_{q3}U_{a2}U_{b2} - U_{a3}U_{b3}U_{p2}U_{q2}}{U_{a1}U_{b1}U_{p2}U_{q2} - U_{a2}U_{b2}U_{p1}U_{q1}} \right|, \quad (17)$$

$$\alpha = -\frac{1}{2} \arg \left(\frac{U_{p2}U_{q2}U_{a3}U_{b3} - U_{a2}U_{b2}U_{p3}U_{q3}}{U_{a1}U_{b1}U_{p3}U_{q3} - U_{a3}U_{b3}U_{p1}U_{q1}} \right) \quad (18)$$

and

$$\beta = -\frac{1}{2} \arg \left(\frac{U_{p3}U_{q3}U_{a2}U_{b2} - U_{a3}U_{b3}U_{p2}U_{q2}}{U_{a1}U_{b1}U_{p2}U_{q2} - U_{a2}U_{b2}U_{p1}U_{q1}} \right) - \delta. \quad (19)$$

Eqs. (18) and (19) give the Majorana phases α and β in terms of θ_{13} and δ since θ_{12} and θ_{23} are known experimentally. Similarly, Eqs. (16) and (17) give the mass ratios $\left(\frac{m_1}{m_2}, \frac{m_1}{m_2}\right)$ as functions of θ_{13} and δ . Since, Δm_{12}^2 and Δm_{23}^2 are known experimentally, the values of mass ratios $\left(\frac{m_1}{m_2}, \frac{m_1}{m_2}\right)$ from Eqs. (16) and (17) can be used to calculate m_1 . This can be done by inverting Eqs. (12) and (13) to obtain the two values of m_1 , viz.

$$m_1 = \left(\frac{m_1}{m_2}\right) \sqrt{\frac{\Delta m_{12}^2}{1 - \left(\frac{m_1}{m_2}\right)^2}} \quad (20)$$

and

$$m_1 = \left(\frac{m_1}{m_3}\right) \sqrt{\frac{\Delta m_{12}^2 + \Delta m_{23}^2}{1 - \left(\frac{m_1}{m_3}\right)^2}}, \quad (21)$$

The two values of m_1 obtained above from the mass ratios $\left(\frac{m_1}{m_2}\right)$ and $\left(\frac{m_1}{m_2}\right)$, respectively, must be equal. Thus, we can constrain (θ_{13}, δ) plane using the experimental inputs for Δm_{12}^2 , Δm_{23}^2 , θ_{12} and θ_{23} . The Dirac-type CP violating phase, δ , is given full variation from 0° to 360° and θ_{13} is varied from zero to its upper bound from CHOOZ experiment. We impose the constraint that the two values of m_1 given by Eqs. (20) and (21) must be equal to constrain (θ_{13}, δ) plane. We use the current best fit values of the oscillation parameters with 1σ (3σ) [9] errors given below:

$$\begin{aligned} \Delta m_{12}^2 &= 7.9_{-0.3(0.8)}^{+0.3(1.0)} \times 10^{-5} eV^2, \\ \Delta m_{23}^2 &= \pm 2.2_{-0.27(0.8)}^{+0.37(1.1)} \times 10^{-3} eV^2, \end{aligned}$$

$$\begin{aligned}
s_{12}^2 &= 0.31_{-0.03(0.07)}^{+0.02(0.09)}, \\
s_{23}^2 &= 0.50_{-0.05(0.16)}^{+0.06(0.18)}, \\
s_{13}^2 &< 0.012(0.046).
\end{aligned}
\tag{22}$$

Here, '+' ('-') sign with the value of Δm_{23}^2 is for normal (inverted) hierarchy. We also calculate the Jarlskog rephasing invariant quantity [10]

$$J = s_{12}s_{23}s_{13}c_{12}c_{23}c_{13}^2 \sin \delta \tag{23}$$

for the allowed parameter space.

In our numerical analysis outlined above, the two squared-mass differences (Δm_{12}^2 and Δm_{23}^2) enter as two independent experimental inputs while the earlier analyses [1, 2, 3] require the ratio of two known mass-squared differences

$$R_\nu \equiv \frac{\Delta m_{12}^2}{\Delta m_{23}^2} = \frac{1 - \left(\frac{m_1}{m_2}\right)^2}{\left|1 - \frac{\left(\frac{m_1}{m_2}\right)^2}{\left(\frac{m_1}{m_3}\right)^2}\right|} \tag{24}$$

to lie in the experimentally allowed range in order to constrain the other neutrino parameters. Our analysis makes direct use of the two mass-squared differences and has more constraining power whereas the earlier analyses which make the use of the ratio R_ν loose some of the constraining power because this procedure does not use the full experimental information currently available with us in the shape of two mass-squared differences. Moreover, since R_ν is a function of mass ratios, it does not depend upon the absolute neutrino mass scale. It is obvious that the two mass ratios $\left(\frac{m_1}{m_2}\right)$ and $\left(\frac{m_1}{m_3}\right)$ may yield the experimentally allowed values of R_ν [Eq. (25)] but give mutually inconsistent values of m_1 [Eqs. (20) and (21)]. Such mass ratios will be allowed in an analysis based upon R_ν [1, 2, 3]. However, our analysis selects only those mass ratios for which the values of m_1 obtained from Eqs. (20) and (21) are identical and R_ν for these values of the mass ratios is automatically limited to be within the allowed experimental range. Moreover, the definition of R_ν

$$R_\nu \equiv \frac{\Delta m_{12}^2}{\Delta m_{23}^2} = \frac{|m_2^2 - m_1^2|}{|m_3^2 - m_2^2|} \tag{25}$$

used in many earlier analyses does not make use of the knowledge of solar mass hierarchy which is already known to constrain the neutrino parameter space. Our analysis disallows the the class D of two-texture zero neutrino mass matrices which has been allowed marginally by Guo and Xing [3].

4 Results and discussion

In this section, we shall present the results of our numerical analysis for neutrino mass matrices of classes A, B and C based upon the approach described in the previous section. However, it will be helpful to know the Tayler series expansions of Eqs. (16-19) to appreciate the numerical results. We perform Taylor series expansions of of Eqs. (16-19) in the powers of s_{13} and tabulate the zeroth order terms in Table 2.

Type	$\frac{m_1}{m_2}$	$\frac{m_1}{m_3}$	α	β
A_1	$\tan^2 \theta_{12}$	$\tan \theta_{12} \tan \theta_{23} \sin \theta_{13}$	$n + \frac{1}{2}\pi$	$\beta + \frac{\delta}{2} = n\pi$
A_2	$\tan^2 \theta_{12}$	$\frac{\tan \theta_{12} \sin \theta_{13}}{\tan \theta_{23}}$	$n + \frac{1}{2}\pi$	$\beta + \frac{\delta}{2} = (n + \frac{1}{2})\pi$
B_1	1	$\tan^2 \theta_{23}$	$n\pi$	$\beta + \delta = (n + \frac{1}{2})\pi$
B_2	1	$\frac{1}{\tan^2 \theta_{23}}$	$n\pi$	$\beta + \delta = (n + \frac{1}{2})\pi$
B_3	1	$\tan^2 \theta_{23}$	$n\pi$	$\beta + \delta = (n + \frac{1}{2})\pi$
B_4	1	$\frac{1}{\tan^2 \theta_{23}}$	$n\pi$	$\beta + \delta = (n + \frac{1}{2})\pi$
C	$\frac{1}{\tan^2 \theta_{12}}$	$\frac{1}{\tan \theta_{12} \tan 2\theta_{23} \sin \theta_{13}}$	$n + \frac{1}{2}\pi$	
D_1	$\frac{1}{\tan^2 \theta_{12}}$	$\frac{\tan \theta_{23}}{\tan \theta_{12} \sin \theta_{13}}$	$n\pi$	$\beta + \frac{\delta}{2} = (n + \frac{1}{2})\pi$
D_2	$\frac{1}{\tan^2 \theta_{12}}$	$\frac{1}{\tan \theta_{23} \tan \theta_{12} \sin \theta_{13}}$	$n + \frac{1}{2}\pi$	$\beta + \frac{\delta}{2} = n\pi$

Table 2: Zeroth order approximations for neutrino mass matrices with two texture zeros.

C.L.	$m_1(10^{-3}eV)$	$\alpha(\text{deg})$	$\beta(\text{deg})$	$\theta_{13}(\text{deg})$	J
1	2.8 - 4.2	83.4 - 96.6	-59.4 - 59.4	5.6 - 6.3	-0.011 - 0.011
2	2.0 - 10.0	76.4 - 103.6	-90 - 90	4.6 - 9.8	-0.021 - 0.021
3	1.6 - 16.2	71.2 - 108.8	-90 - 90	3.5 - 12.4	-0.046 - 0.046

Table 3: The predictions for neutrino mass matrices of class A.

4.1 Class A

It can be seen from Table 2 that both the mass ratios $\frac{m_1}{m_2}$ and $\frac{m_1}{m_3}$ are much smaller than one for neutrino mass matrices of class A. So, neutrino mass matrices of class A give hierarchical spectrum of neutrino masses. This case has, already, been analyzed analytically by us [5] and, here, we shall discuss only the results for the sake of completeness. The agreement between the analytical results reported in the earlier work [5] and the numerical results reported in this work shows the validity of our numerical method described in the last section.

The results for m_1 , α , β , θ_{13} and J for class A mass matrices have been summarized in Table 1 at various confidence levels. These quantities are the same for mass matrices of types A_1 and A_2 . It can be seen from Table 1 that the 3σ lower bound on θ_{13} is 3.5° . The range for the Majorana-type CP-violating phase β at 1σ C.L. is found to be $-59.4^\circ - 59.4^\circ$. However, if the neutrino oscillation parameters are allowed to vary beyond their present 1.2σ C.L. ranges, the full range for β ($-90^\circ - 90^\circ$) is allowed. As noted earlier, the neutrino mass matrices of type A_1 and A_2 differ in their predictions for δ and θ_{23} . At one standard deviation, the allowed range of δ is ($-110.8^\circ - 110.8^\circ$) for type A_1 and ($69.2^\circ - 290.8^\circ$) for type A_2 and the allowed range of θ_{23} is ($44.0^\circ - 48.2^\circ$) for type A_1 and ($41.8^\circ - 46.0^\circ$) for type A_2 [Table 2]. Just like β , no constraint on δ is obtained above 1.2σ C.L. The neutrino mass matrices of types A_1 and A_2 have some overlap in their predictions regarding δ and θ_{23} at one standard deviation. Therefore, a precise measurement of the oscillation parameters is necessary to distinguish the neutrino mass matrices of types A_1 and A_2 .

1 σ predictions	δ	θ_{23}
A_1	$-110.8^\circ - 110.8^\circ$	$44.0^\circ - 48.2^\circ$
A_2	$69.2^\circ - 290.8^\circ$	$41.8^\circ - 46.0^\circ$

Table 4: The predictions for δ and θ_{23} for neutrino mass matrices of types A_1 and A_2 .

In Fig. 1 (identical for A_1 and A_2), we depict the allowed values of m_1 , α and β as the correlation plots at one standard deviation. The upper panel shows α as a function of m_1 and the lower panel shows β as a function of α . The large spread in the (m_1, α) plot is due to the errors in the neutrino oscillation parameters. The two Majorana phases are strongly correlated with each other. Such a correlation between the Majorana phases was noted earlier by Xing [2, 3]. However, full ranges $(-90^\circ - 90^\circ)$ are allowed for the two Majorana phases in that analysis [3]. In contrast, we obtain a very narrow range for the Majorana phase α around 90° [Table 3]. Similarly, the Majorana phase β is, also, constrained if the oscillation parameters are limited to their 1σ ranges. We have, also, plotted J as a function of m_1 in Fig. 1 where it can be seen that J is not equal to zero and neutrino mass matrices of class A are necessarily CP-violating.

In Fig. 2, we depict the correlation plots of α and β with δ for matrices of type A_1 (left panel) and A_2 (right panel). We, also, show the correlation plots of δ and θ_{23} with one another as well as with θ_{13} in Fig. 2. The Dirac-type CP-violating phase δ is strongly correlated with the Majorana-type CP-violating phases α and β [Cf. Table 4]. It can be seen from (α, δ) and (β, δ) correlation plots that there are small deviations in the values of α around 90° and the correlation between β and δ is almost linear. The fact that $\beta + \frac{\delta}{2} = 0$ for mass matrices of type A_1 and $\beta + \frac{\delta}{2} = \frac{1}{2}$ mass matrices of type A_2 is apparent from the (β, δ) correlation plots given in the left and right panels in Fig. 2, respectively. The (β, δ) correlation was noted earlier by Xing [2] in its approximate form in a different parameterization. The (δ, θ_{23}) plots, clearly, illustrate the point that the neutrino mass matrices of type A_1 and A_2 have different predictions for these variables [Table 4] and only a limited region is allowed on the (δ, θ_{23}) plane. This is contrary to the analysis done by Guo and Xing [3] where no constraints on δ and θ_{23} have been obtained. In fact, this feature is crucial for distinguishing mass matrices of type A_1 and A_2 which were found to be degenerate in the earlier analyses [1, 2, 3]. The constraints on δ and θ_{23} are very sensitive to the values of θ_{13} . For the values of θ_{13} smaller than 1σ CHOOZ bound, the constraints on δ and θ_{23} become stronger which can be seen from the $(\theta_{13}, \theta_{23})$ and (θ_{13}, δ) plots. For example, if $\theta_{13} > 6^\circ$, then $\theta_{23} > 46^\circ$ (above maximal) for type A_1 and $\theta_{23} < 44^\circ$ (below maximal) for type A_2 . It can, also, be seen from the $(\theta_{13}, \theta_{23})$ correlation plot in Fig. 2 that the deviation of θ_{23} from maximality is larger for smaller values of θ_{13} . Therefore, if future experiments measure θ_{13} below its present 1σ bound, the neutrino mass matrices of type A_1 and A_2 will have different predictions for δ and θ_{23} with no overlap. However, it would be difficult to differentiate between matrices of types A_1 and A_2 if θ_{13} is found to be above its present 1σ range. As noted earlier, different quadrants for δ are selected for neutrino mass matrices of type A_1 and A_2 . Fig. 2, also, depicts J as a function of δ for types A_1 (left panel) and A_2 (right panel).

C.L.	α	M_{ee}	J
1 σ	-2.0^0 - 2.0^0	$\geq 0.058eV$	-0.025 - 0.025
2 σ	-8.1^0 - 8.1^0	$\geq 0.030eV$	-0.037 - 0.037
3 σ	-23.7^0 - 23.7^0	$\geq 0.018eV$	-0.05 - 0.05

Table 5: The predictions for neutrino mass matrices of class B.

4.2 Class B

It can be seen from Table 2 that the mass ratios $\frac{m_1}{m_2}$ and $\frac{m_1}{m_3}$ are approximately equal to one for neutrino mass matrices of class B. So, neutrino mass matrices of class B give quasi-degenerate spectrum of neutrino masses. For neutrino mass matrices of class B , the ratio $\frac{m_1}{m_2}$, upto first order in s_{13} , is given by

$$\begin{aligned}
B_1 &: \quad \frac{m_1}{m_2} = 1 + \frac{c_{23}}{c_{12}s_{12}s_{23}^3} s_{13} \cos \delta, \\
B_2 &: \quad \frac{m_1}{m_2} = 1 - \frac{s_{23}}{c_{12}s_{12}c_{23}^3} s_{13} \cos \delta, \\
B_3 &: \quad \frac{m_1}{m_2} = 1 - \frac{c_{23} \tan^2 \theta_{23}}{c_{12}s_{12}s_{23}^3} s_{13} \cos \delta, \\
B_4 &: \quad \frac{m_1}{m_2} = 1 + \frac{s_{23} \cot^2 \theta_{23}}{c_{12}s_{12}c_{23}^3} s_{13} \cos \delta.
\end{aligned} \tag{26}$$

Since, the mass ratio $\frac{m_1}{m_2}$ is always smaller than one, we find that $\cos \delta$ should be negative for B_1 and B_4 and positive for B_2 and B_3 . Hence, B_1 and B_4 (or B_2 and B_3) will have identical predictions for δ . Similarly, it can be seen that B_1 and B_3 (or B_2 and B_4) will have, almost, identical predictions for θ_{23} if it is near maximality. However, B_1 and B_4 (or B_2 and B_3) can be distinguished from each another by their predictions for the deviation of θ_{23} from maximality and B_1 and B_3 (or B_2 and B_4) can be distinguished from each another by their predictions for the quadrant of δ . Thus, the four-fold degeneracy in class B is, now, lifted. Moreover, it follows from Eqs. (25) that the second term should be suppressed by $s_{13} \cos \delta$ if neutrino mass spectrum is quasi-degenerate ($m_1 \sim m_2$). For large θ_{13} , the Dirac phase δ should be peaked around 90^0 or 270^0 to keep $s_{13} \cos \delta$ small. However, for small θ_{13} , no additional constraint on δ is obtained. The fact that $\cos \delta$ is negative for B_1 and B_4 type mass matrices and positive for B_2 and B_3 type mass matrices results in the elimination of two quadrants of delta for each of these subgroups due to the wrong sign of $\cos \delta$. This is contrary to the analyses [2, 3] which do not constrain the Dirac phase δ at all for these subgroup of mass matrices. In the analysis by Xing [2], the mass ratios $\frac{m_1}{m_3}$ and $\frac{m_2}{m_3}$ were examined as a result of which this important constraint on δ coming from the mass ratio $\left(\frac{m_1}{m_2}\right)$ could not be obtained. In the detailed numerical analysis by Guo and Xing [3] based upon R_ν defined in Eq. (25) which does not make use of the solar mass hierarchy, no constraints on δ were obtained for neutrino mass matrices of class B.

Now, we present the numerical results of the analysis for mass matrices of class B. The allowed range of δ is $(90^0 - 270^0)$ for types B_1 and B_4 and $(-90^0 - 90^0)$ for types B_2 and

B_3 . In other words, $\cos \delta$ is negative for types B_1 and B_4 and positive for types B_2 and B_3 , as expected. If $\theta_{23} < 45^\circ$, B_1 and B_3 give normal hierarchy while B_2 and B_4 give inverted hierarchy. Similarly, if $\theta_{23} > 45^\circ$, then B_1 and B_3 give inverted hierarchy while B_2 and B_4 give normal hierarchy. As noted earlier, the four types of neutrino mass matrices within class B differ in their predictions for δ and θ_{23} . There is no lower bound on θ_{13} in class B. The Majorana-type CP-violating phase β , also, remains unconstrained. Full range of θ_{23} (41.8° - 48.2° at 1σ) is allowed for all the four types of neutrino mass matrices. The predictions for α , M_{ee} and J for class B mass matrices have been summarized in Table 5. These quantities are the same for mass matrices of types B_1 , B_2 , B_3 and B_4 . It can be seen that α is restricted to a very small range around zero and definite lower bounds on M_{ee} are obtained. It is important to note that $\theta_{23} = 45^\circ$ is disallowed by the mass matrices of class B.

In Fig. 3, the correlation plots for α , β , δ , θ_{13} , m_1 , M_{ee} and J , which are the same for all eight possible cases of B type mass matrices (B_1 , B_2 , B_3 and B_4 with normal as well as inverted hierarchy), have been shown. These plots show that B type mass matrices exhibit eightfold degeneracy in the sense that eight different types of mass matrices have identical predictions for neutrino parameters except for the signs of $\cos 2\theta_{23}$, $\cos \delta$ and Δm_{23}^2 . This eightfold degeneracy cannot be lifted by vacuum oscillation experiments since the signs of the above three quantities cannot be determined in these experiments. This results in an eightfold degeneracy in the neutrino parameters [11, 12, 13] which is reflected in the eightfold degeneracy of the neutrino mass matrices of class B. The resolution of the eightfold degeneracy in the neutrino parameter space will, also, resolve the eightfold degeneracy of the neutrino mass matrices of class B.

Figures 3(a-d) depict the correlations of α , β , J and M_{ee} with θ_{13} . It can be seen from Fig. 3(a) that an upper bound on θ_{13} constrains α to a very narrow range. Even at three standard deviations, the allowed range of α is $-23.7^\circ \leq \alpha \leq 23.7^\circ$ [Cf. Table 5]. However, no constraints are obtained on the Majorana phase β [Fig. 3(b)]. The correlation plot of J with θ_{13} shows a linear behaviour which is a consequence of θ_{13} being small and δ being near 90° or 270° for most of the allowed points in the neutrino parameter space. Since, $M_{ee} \simeq m_1$, we give the correlation plots for M_{ee} instead of m_1 in Fig. 3(d) where it can be seen that the absolute neutrino mass scale and 1-3 mixing angles are anti-correlated with each other. Next, we depict the correlations of the quantities M_{ee} and J with the Majorana phases α and β in figures 3(e-h). The effective Majorana mass M_{ee} diverges at $\alpha = 0$ and $\beta = 0$ and so these points are not allowed. A lower bound on M_{ee} is required to constrain the Majorana phase β which, otherwise, remains unconstrained for mass matrices of class B [Fig. 3(f)]. It can be seen from Fig. 3(g) that J and α are directly correlated with each other. This is due to the fact that α is constrained to a very small range around zero degree. The correlation between the two Majorana phases α and β is depicted in Fig. 3(i) which shows that β will be nearly zero for large α and vice-versa. Fig. 3(j) depicts the correlation between J and M_{ee} . One can see that maximal CP-violation is possible near the lowest possible value of M_{ee} in class B. The analysis by Guo and Xing [3] fails to obtain any constraints on the ranges of CP-violating phases (α , β and δ) for the reasons discussed earlier.

Fig. 4 depicts the correlations which lift the degeneracy between the neutrino mass matrices

of types B_1 (B_4) and B_2 (B_3). Since, the range of Dirac-type CP-violating phase, δ , is different for B_1 (B_4) and B_2 (B_3), the eightfold degeneracy in B type mass matrices has been reduced to four-fold. The left panel depicts the correlation plots for both B_1 and B_4 and the right panel depicts the correlation plots for B_2 and B_3 . It can be seen from Fig. 4(a,b) that the range of Dirac-type CP-violating phase, δ , is $90^\circ \leq \delta \leq 270^\circ$ ($-90^\circ \leq \delta \leq 90^\circ$) for B_1 and B_4 (B_2 and B_3) type mass matrices. Also, there is a strong correlation between Majorana-type CP violating phase, β , and Dirac-type CP-violating phase, δ reinforcing the zeroth order result ($\beta + \delta = (n + \frac{1}{2})\pi$) given in Table 2. It can be seen from Fig. 4(c,d) that θ_{13} remains unconstrained in all cases because full range of θ_{13} is allowed at $\delta = 90^\circ$ and 270° . However, as we deviate from these values of δ , θ_{13} decreases rapidly to very small values. So, if the CP violation is found to be non-maximal, θ_{13} will be constrained to very small values. However, if CP violation is found to be nearly maximal, θ_{13} can be large. Thus, the suppression factor $s_{13}\delta$ in the first order correction in the Taylor expansion for $\left(\frac{m_1}{m_2}\right)$ is small which reinforces the validity of the zeroth order approximation for this class.

Fig. 5 depicts the correlations of M_{ee} and α with θ_{23} . The correlation plots with θ_{23} can be used to further reduced the remaining four-fold degeneracy in B type mass matrices to a two-fold degeneracy which will be lifted by the determination of the neutrino mass hierarchy. The left panel (right panel) depicts the correlation plots for $B_1(NH)$ and $B_2(IH)$ ($B_1(IH)$ and $B_2(NH)$). The correlation plots of M_{ee} and α with θ_{23} for $B_3(NH)$ and $B_4(IH)$ (or $B_3(IH)$ and $B_4(NH)$) will be, almost, identical to the plots given in Fig. 5 because B_1 and B_3 (or B_2 and B_4) have, almost, identical predictions for θ_{23} and, therefore, are not given here. It can be seen from Fig. 5(a,b) that the effective Majorana mass M_{ee} is strongly correlated with θ_{23} . Moreover, maximal value of θ_{23} is not allowed by the current neutrino oscillation data since M_{ee} diverges at $\theta_{23} = \frac{\pi}{4}$. Larger the deviation of θ_{23} from maximality, smaller is the value of M_{ee} . Also, a large value of α implies large deviations in θ_{23} from maximality. The deviation of 2-3 mixing from maximality is an important feature of neutrino mass matrices of class B which results from an upper bound on M_{ee} . Moreover, this prediction is also linked to the interplay between the hierarchy and the quadrant of δ .

Figures 4 and 5 illustrate the decoupling of degeneracies in the sense that two mass matrices can be degenerate in their δ predictions but may have different predictions for θ_{23} or vice-versa. A similar decoupling of degeneracies occur in neutrino oscillation experiments with matter effects [13] where an experiment may be insensitive to the sign of $\cos \delta$ but can resolve the degeneracy in the sign of $\cos 2\theta_{23}$ or it can be insensitive to the sign of $\cos 2\theta_{23}$ but can resolve the degeneracy in the sign of $\cos \delta$.

4.3 Class C

It can be seen from Table 2 that the mass ratio $\frac{m_1}{m_2}$ is greater than one at zeroth order. However, the higher order terms in the Taylor series expansion of the ratio $\frac{m_1}{m_2}$ may make it smaller than one. Detailed numerical analysis shows that this actually happens and the mass matrices of class C are marginally allowed. The Taylor series expansion for $\frac{m_1}{m_2}$ to the

	β	J	M_{ee}
1 σ	$-15.0^0-15.0^0$	$-0.025-0.025$	≥ 0.020 eV
2 σ	$-16.7^0-16.7^0$	$-0.037-0.037$	≥ 0.013 eV
3 σ	$-18.3^0-18.3^0$	$-0.046-0.046$	≥ 0.008 eV

Table 6: The predictions for β , J and M_{ee} for neutrino mass matrices of class C.

first order in s_{13} is given by

$$\frac{m_1}{m_2} = \frac{1}{\tan^2 \theta_{12}} \left(1 - \frac{\tan 2\theta_{23}}{s_{12}c_{12}} s_{13} \cos \delta \right) \quad (27)$$

For $\frac{m_1}{m_2}$ to be smaller than one, the term $(\tan 2\theta_{23} \cos \delta)$ should be positive. Therefore, when $\theta_{23} < 45^0$, we must have $-90^0 < \delta < 90^0$. Similarly, when $\theta_{23} > 45^0$, we must have $90^0 < \delta < 270^0$. The points $\delta = 90^0$, 270^0 and $\theta_{13} = 0^0$ are not allowed because the first order correction term vanishes at these points. The mixing angle θ_{23} should approach 45^0 as δ approaches 90^0 or 270^0 and θ_{13} approaches 0^0 so that the term $(s_{13} \tan 2\theta_{23} \cos \delta)$ can make the ratio $\frac{m_1}{m_2}$ smaller than one. The mass ratio $\frac{m_1}{m_3}$ is greater than one at the zeroth order. Therefore, neutrino mass matrices of type C should be consistent with inverted hierarchy only. However, we shall see in the detailed numerical analysis that the normal hierarchy is also allowed marginally.

For mass matrices of type C, with inverted hierarchy, the allowed ranges for the parameters β , J and M_{ee} are given in Table 6. All other parameter ranges remain unconstrained. The correlation plots between various plots have been depicted in Figs. 6-8. In Fig. 6, we have given the correlations of α , β , θ_{13} , θ_{23} , M_{ee} and J with δ . As discussed earlier, the values $\delta = 90^0$ and 270^0 are not allowed [Fig. 6a()). Therefore, maximal CP-violation is not allowed for mass matrices of class C. For the maximal values of δ , α should be equal to zero. Therefore, the point $\alpha = 0^0$ is, also, not allowed. However, all other values of α are allowed. It can be seen from the Fig. 6(b) that the correlation plot that β is a periodic function of δ with a period of 180^0 and β can be zero at $\delta = 0^0$ or 180^0 . However, the points $(\beta = 0^0, \delta = 90^0)$ and $(\beta = 0^0, \delta = 270^0)$ are disallowed. The correlation between δ and θ_{13} has been depicted in Fig. 6(c). The correlation between δ and θ_{23} has been depicted in Fig. 6(d) where it can be seen that the maximal 2-3 mixing is not allowed. However, the mixing angle θ_{23} will be below maximality if $\cos \delta$ is positive (-90^0-90^0) and above maximality if $\cos \delta$ is negative (90^0-270^0). These points are, completely, in accordance with the results obtained from the Taylor series expansion. Fig. 6(e) depicts the correlation between M_{ee} and δ . The neutrino mass matrices of class C give a lower bound (about 0.02 eV) on M_{ee} for $\delta = 0^0$ or 180^0 . As δ deviates from the values 0^0 and 180^0 , M_{ee} increases and diverges as δ becomes maximal. The correlation between J and δ has been shown in Fig. 6(f).

In Fig. 7, we have shown the correlations of α , β , θ_{23} and J with θ_{13} . In Fig. 7(a), (θ_{13}, α) correlation has been depicted. Full range (-90^0-90^0) for α is allowed at $\theta_{13} = 0$. However, it can be seen from Fig. 7(a) that a lower bound on θ_{13} of about 4^0 will constrain α to the range (-65^0-65^0) . As we have seen already, β is already constrained to a small range around zero. However, it can be seen from Fig. 7(b) that β can be further constrained if θ_{13}

is found to be larger than 3° . A lower bound on θ_{13} larger than 3° will reject a finite range of β around zero. From the $(\theta_{13}, \theta_{23})$ correlation plot [Fig. 7(c)], it can be seen that larger the value of θ_{13} , larger will be the deviation of θ_{23} from maximality. The point $(\theta_{13} = 0^\circ, \theta_{23} = 45^\circ)$ is not allowed. The disallowed range of θ_{23} around 45° increases with increase in θ_{13} . For example, the disallowed range of θ_{23} at $\theta_{13} = 6^\circ$ is approximately $44^\circ - 46^\circ$. For small values of θ_{13} , J is proportional to θ_{13} and the constant of proportionality is determined by $\sin \delta$ [Cf. Eq. (23)]. These features can be seen graphically in the correlation plot between J and θ_{13} depicted in Fig. 7d.

Some other important correlation plots have been shown in Fig. 8. It can be seen from the (α, β) correlation plot [Fig. 8(a)] that the two Majorana phases can not vanish simultaneously. Moreover, α should be positive if β is negative and vice-versa. The correlation between M_{ee} and α has been shown in Fig. 8(c) where it can be seen that an upper bound on M_{ee} will reject a considerable range of α . The (M_{ee}, β) correlation plot has been given in Fig. 8(d). It can be seen that the allowed range of β (which is $-15^\circ - 15^\circ$ for low value of M_{ee}) can be further constrained if M_{ee} is found to be larger than 0.03 eV. Fig. 8(e) depicts the correlation between M_{ee} and θ_{23} . It can be seen that M_{ee} diverges at maximal 2-3 mixing. An lower bound on M_{ee} can be used to constrain θ_{23} .

For C type mass matrices, with normal hierarchy Dirac-type CP-violation phase, δ , can take only two values, $\delta = 90^\circ$ or 180° . Majorana-type CP-violating phases (α and β) and θ_{13} remain unconstrained. There is a strong correlation between θ_{13} and θ_{23} in this case. Larger the allowed range of θ_{13} , larger will be the deviation of θ_{23} from maximality.

5 Conclusions

If neutrinoless double beta decay searches give positive results and M_{ee} is measured experimentally or the atmospheric/reactor neutrino oscillation experiments confirm inverted hierarchy, the neutrino mass matrices of class A will be ruled out. A generic prediction of this class of models is a lower bound on θ_{13} [Table 1]. If the forthcoming neutrino oscillation experiments measure θ_{13} below 3.5° , the neutrino mass matrices of class A will, again, be ruled out. If M_{ee} is found to be non-zero, the mass matrices of class B or C may be allowed.

The forthcoming neutrino experiments will aim at measuring the Dirac type CP violating phase δ and the deviations of the atmospheric mixing angle from maximality [14]. The results of these experiments will fall in one of the following eight categories of phenomenological interest:

1. NH, $\theta_{23} < 45^\circ$ and $90^\circ < \delta < 270^\circ$,
2. NH, $\theta_{23} > 45^\circ$ and $-90^\circ < \delta < 90^\circ$,
3. NH, $\theta_{23} < 45^\circ$ and $-90^\circ < \delta < 90^\circ$,
4. NH, $\theta_{23} > 45^\circ$ and $90^\circ < \delta < 270^\circ$,
5. IH, $\theta_{23} > 45^\circ$ and $90^\circ < \delta < 270^\circ$.

Categories	Degeneracies			Matrices		
	$sgn\Delta m_{23}^2$	$sgn \cos 2\theta_{23}$	$sgn \cos \delta$	A	B	C
1	+	+	−	A_2	$B_1(NH)$	\times
2	+	−	+	A_1	$B_2(NH)$	\times
3	+	+	+	\times	$B_3(NH)$	\times
4	+	−	−	\times	$B_4(NH)$	\times
5	−	−	−	\times	$B_1(IH)$	\times
6	−	+	+	\times	$B_2(IH)$	$C(IH)$
7	−	−	+	\times	$B_3(IH)$	$C(NH)$
8	−	+	−	\times	$B_4(IH)$	\times

Table 7: The consequences of resolving the eightfold experimental degeneracies for the neutrino mass matrices with two texture zeros.

6. IH, $\theta_{23} < 45^0$ and $-90^0 < \delta < 90^0$,
7. IH, $\theta_{23} > 45^0$ and $-90^0 < \delta < 90^0$,
8. IH, $\theta_{23} < 45^0$ and $90^0 < \delta < 270^0$,

In fact, the above eight possibilities cannot be distinguished from one another in the absence of matter effects. This eightfold degeneracy is well known in the literature and the ways to resolve it have been studied extensively. The degeneracy occurs because vacuum oscillations are not affected by the signs of Δm_{23}^2 , $\sin 2\theta_{23}$ and $\cos \delta$. Since the matter effect are sensitive to these signs, the eightfold degeneracy can be resolved [11, 12, 13]. The resolution of the eightfold degeneracy will also resolve the two-fold degeneracy in mass matrices of class A and eightfold degeneracy in mass matrices of class B. The consequences of the resolving the eightfold degeneracy in the neutrino parameter space for two-texture zero neutrino mass matrices have been summarized in Table 7.

If the neutrino mass matrices with two texture zeros are confirmed experimentally, the CP-violation in lepton number conserving and non-conserving processes will be correlated in a definite way and there will be only one independent CP-violating measure for both types of processes.

6 Acknowledgments

The research work of S. D. and S. V. is supported by the Board of Research in Nuclear Sciences (BRNS), Department of Atomic Energy, Government of India *vide* Grant No. 2004/37/23/BRNS/399. S. K. acknowledges the financial support provided by Council for Scientific and Industrial Research (CSIR), Government of India. We would like to thank Manmohan Gupta for critical reading of the manuscript and helpful suggestions.

References

- [1] Paul H. Frampton, Sheldon L. Glashow and Danny Marfatia, *Phys. Lett.* **B 536**, 79 (2002); Bipin R. Desai, D. P. Roy and Alexander R. Vaucher, *Mod. Phys. Lett* **A 18**, 1355 (2003).
- [2] Zhi-zhong Xing, *Phys. Lett.* **B 530** 159 (2002).
- [3] Wanlei Guo and Zhi-zhong Xing, *Phys. Rev.* **D 67**, 053002 (2003).
- [4] Alexander Merle and Werner Rodejohann, *Phys. Rev.* **D 73**, 073012 (2006); S. Dev and Sanjeev Kumar, hep-ph/0607048.
- [5] S. Dev, Sanjeev Kumar, Surender Verma and Shivani Gupta, hep-ph/0611313.
- [6] G. C. Branco, R. Gonzalez Felipe, F. R. Joaquim and T. Yanagida, *Phys. Lett.* **B 562** 265 (2003); Bhag C. Chauhan, Joao Pulido and Marco Picariello, *Phys. Rev.* **D 73**, 053003 (2006).
- [7] Xiao-Gang He and A. Zee, hep-ph/0302201 v2.
- [8] G. L. Fogli *et al*, [arXiv:hep-ph/0506083 v1].
- [9] M. Maltony, T. Schwetz, M. A. Tortola and J. W. F. Valle, *New J. Phys.* **6**, 122 (2004).
- [10] C. Jarlskog *Phys. Rev. Lett.* **55**, 1039 (1985).
- [11] V. Barger, D. Marfatia and K. Whisnant, hep-ph/0112119 v1.
- [12] Hisakazu Minakata, Hiroshi Nunokawa, Stephen Parke, hep-ph/0208163 v2.
- [13] Takaaki Kajita, Hisakazu Minakata, Shoei Nakayama, and Hiroshi Nunokawa, hep-ph/0609286.
- [14] E. Abouzaid *et al*, Report of the APS Neutrino Study Reactor Working Group, 2004.

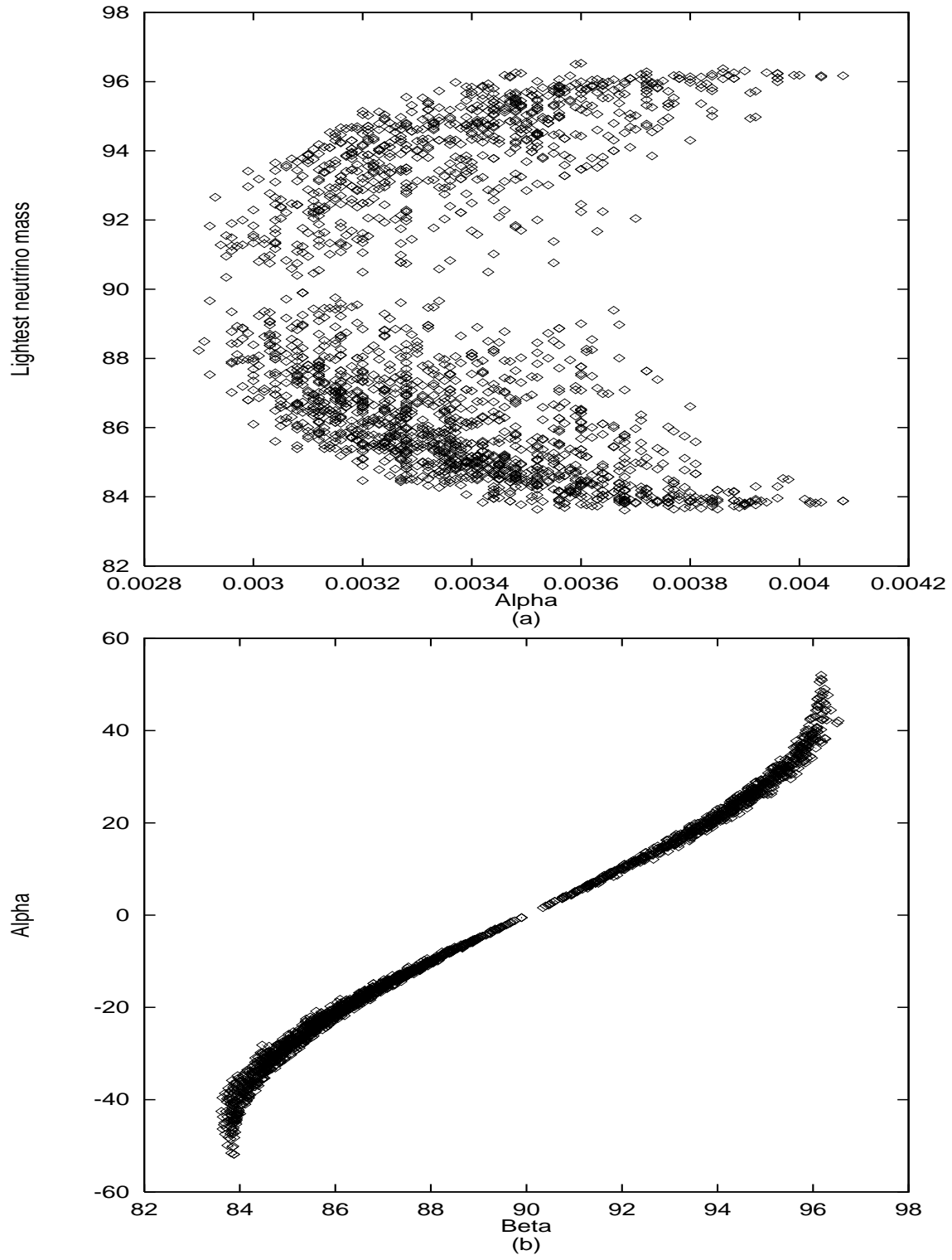


Figure 1: Correlation plots for neutrino mass matrices of class A at one standard deviation.

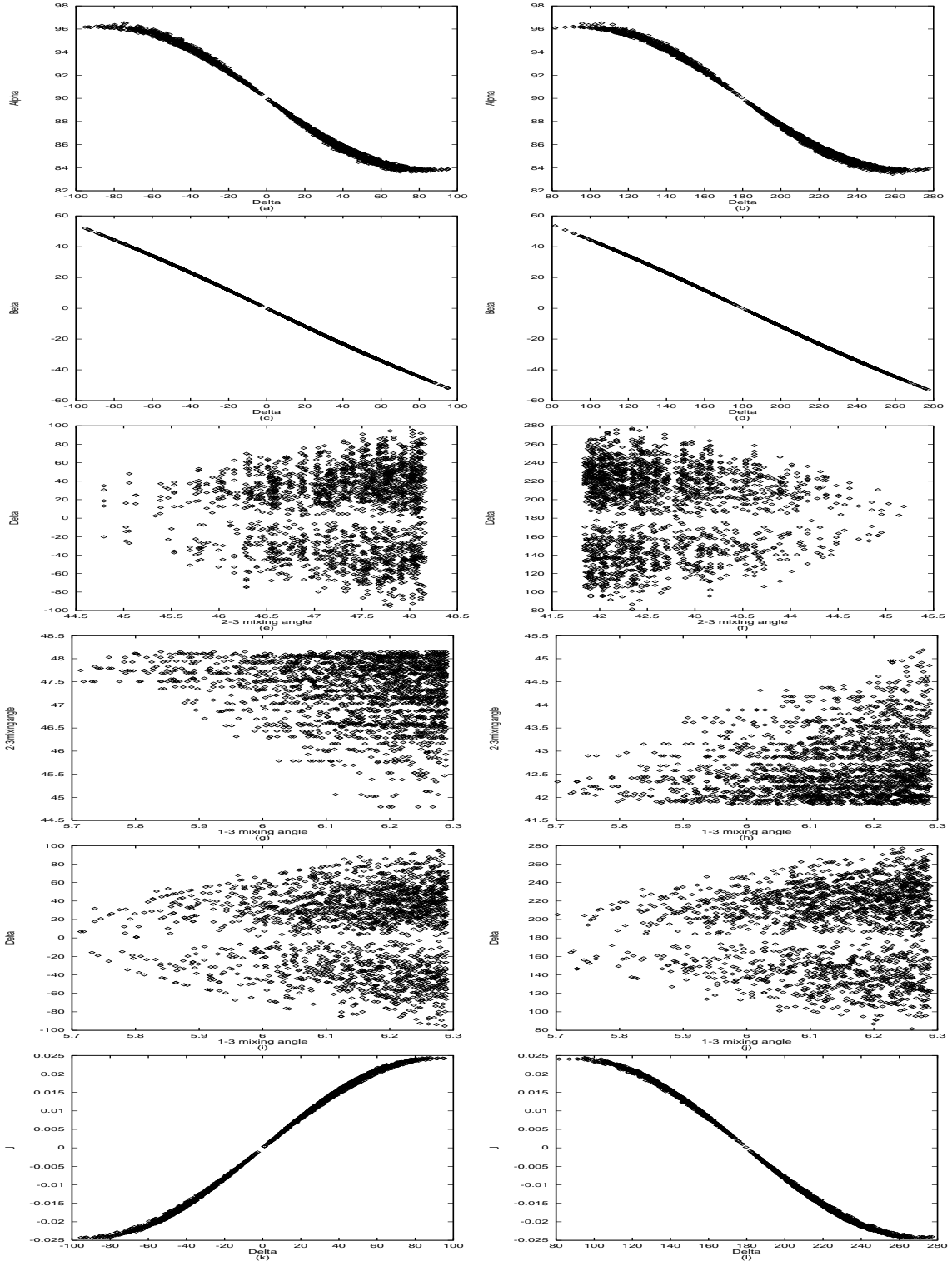


Figure 2: Correlation plots for neutrino mass matrices of type A_1 (left panel) and A_2 (right panel).

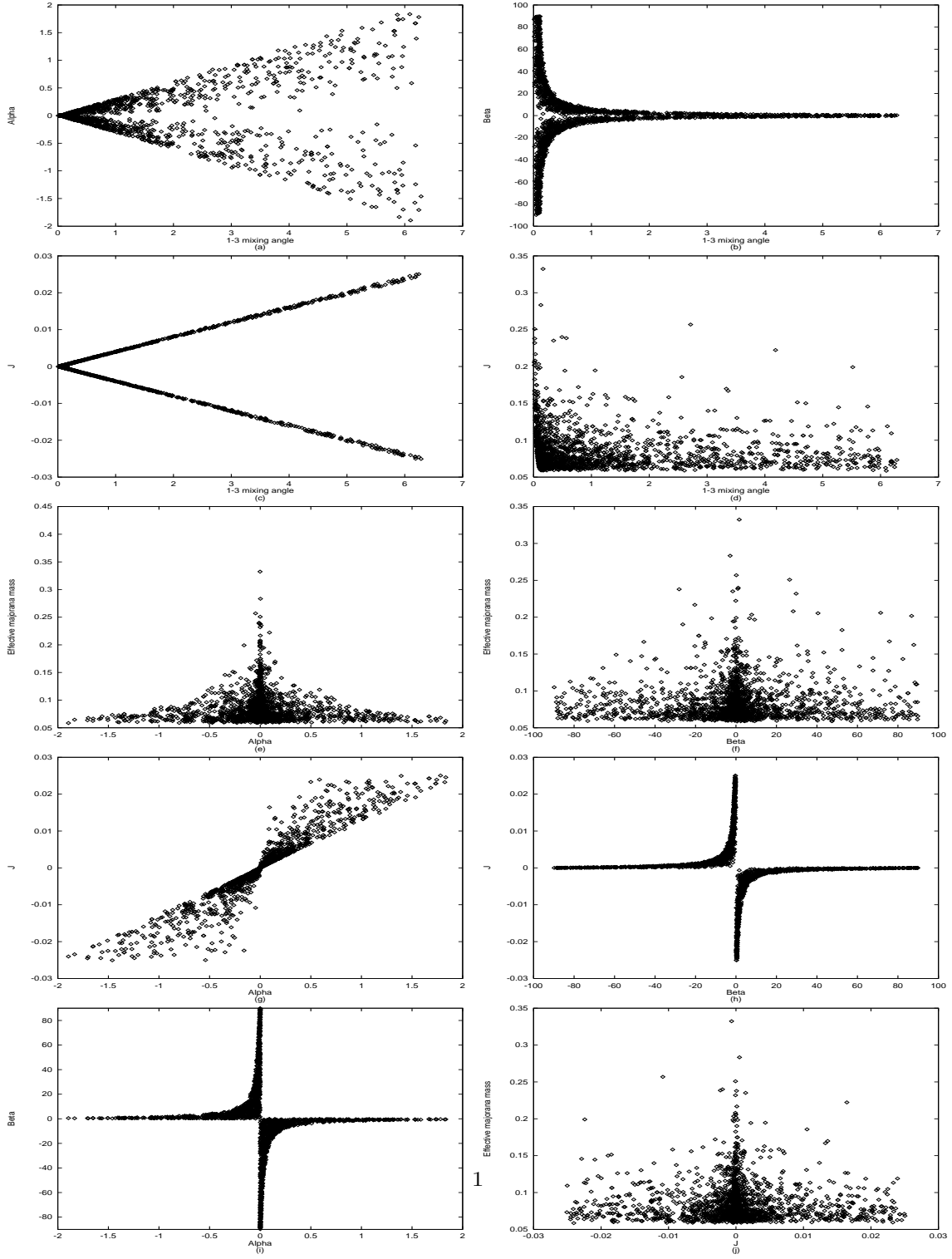


Figure 3: 1σ correlation plots for B_1 , B_2 , B_3 and B_4 type mass matrices with normal as well as inverted hierarchies.

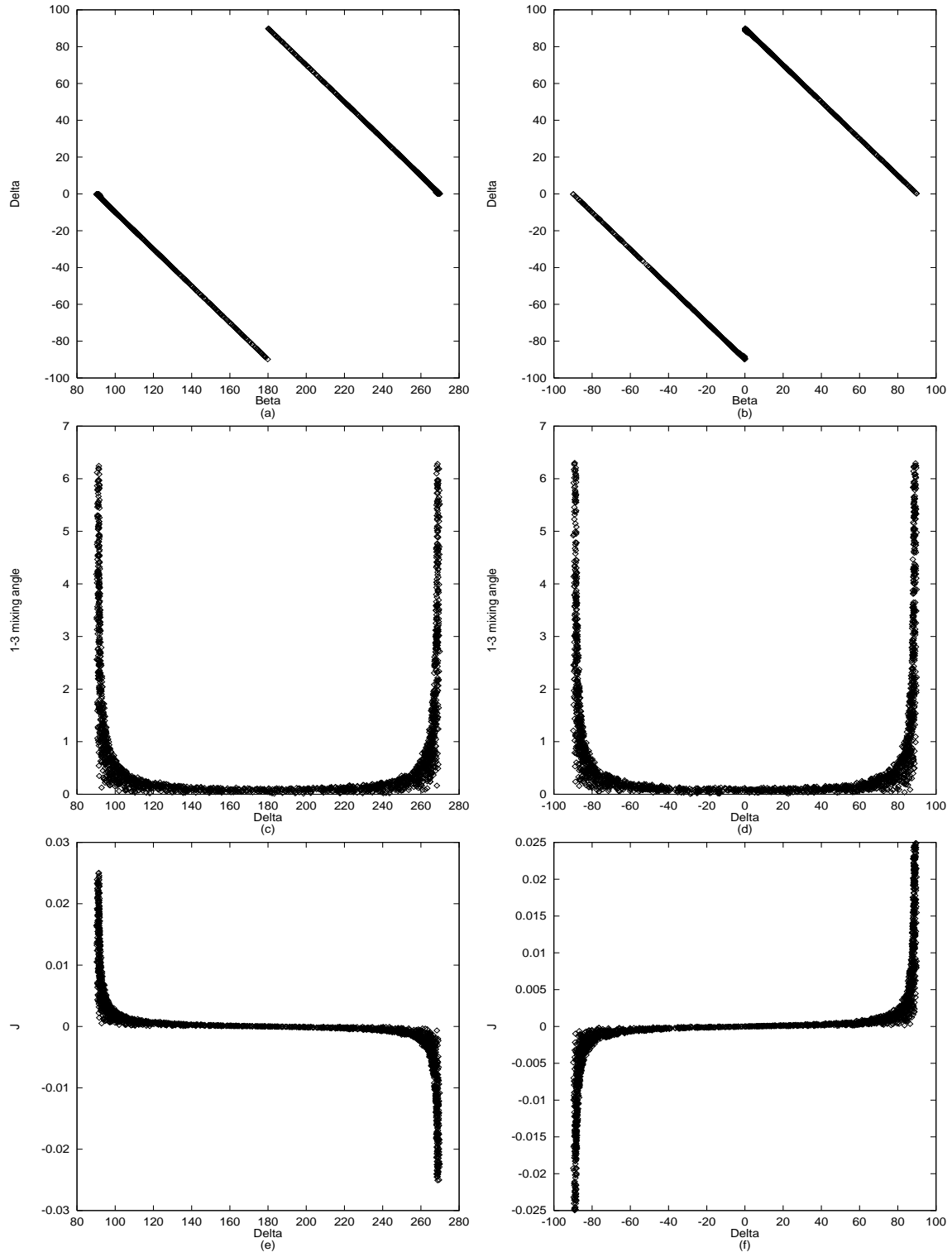


Figure 4: The left panel shows the correlation plots for B_1 or B_4 while right panel shows the correlation plots for B_2 or B_3 type mass matrices.

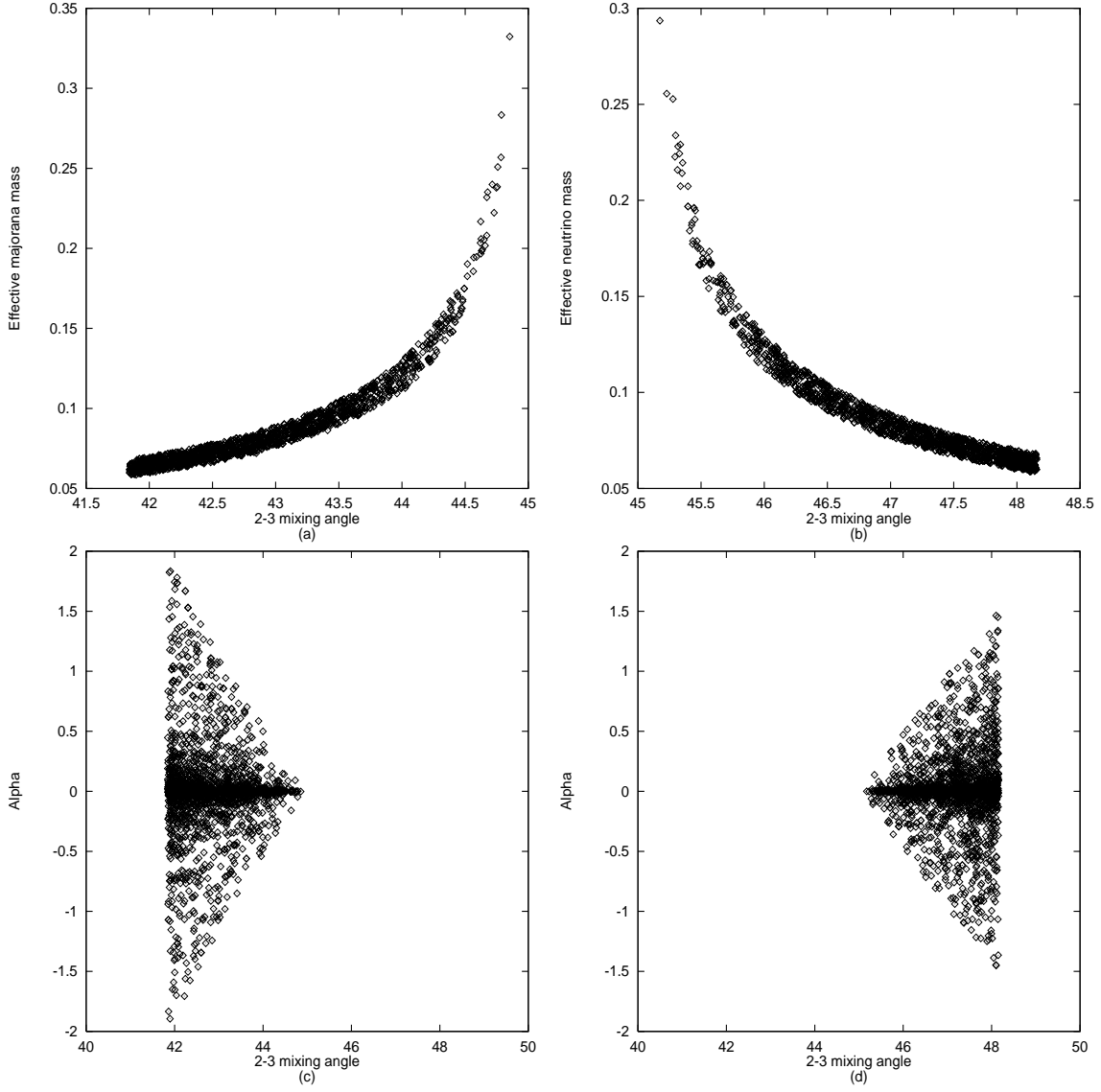


Figure 5: Variation of M_{ee} and α with θ_{23} . The left [right] panel plots are for $B_1(NH)$, $B_2(IH)$ [$B_3(IH)$, $B_4(NH)$] type mass matrices.

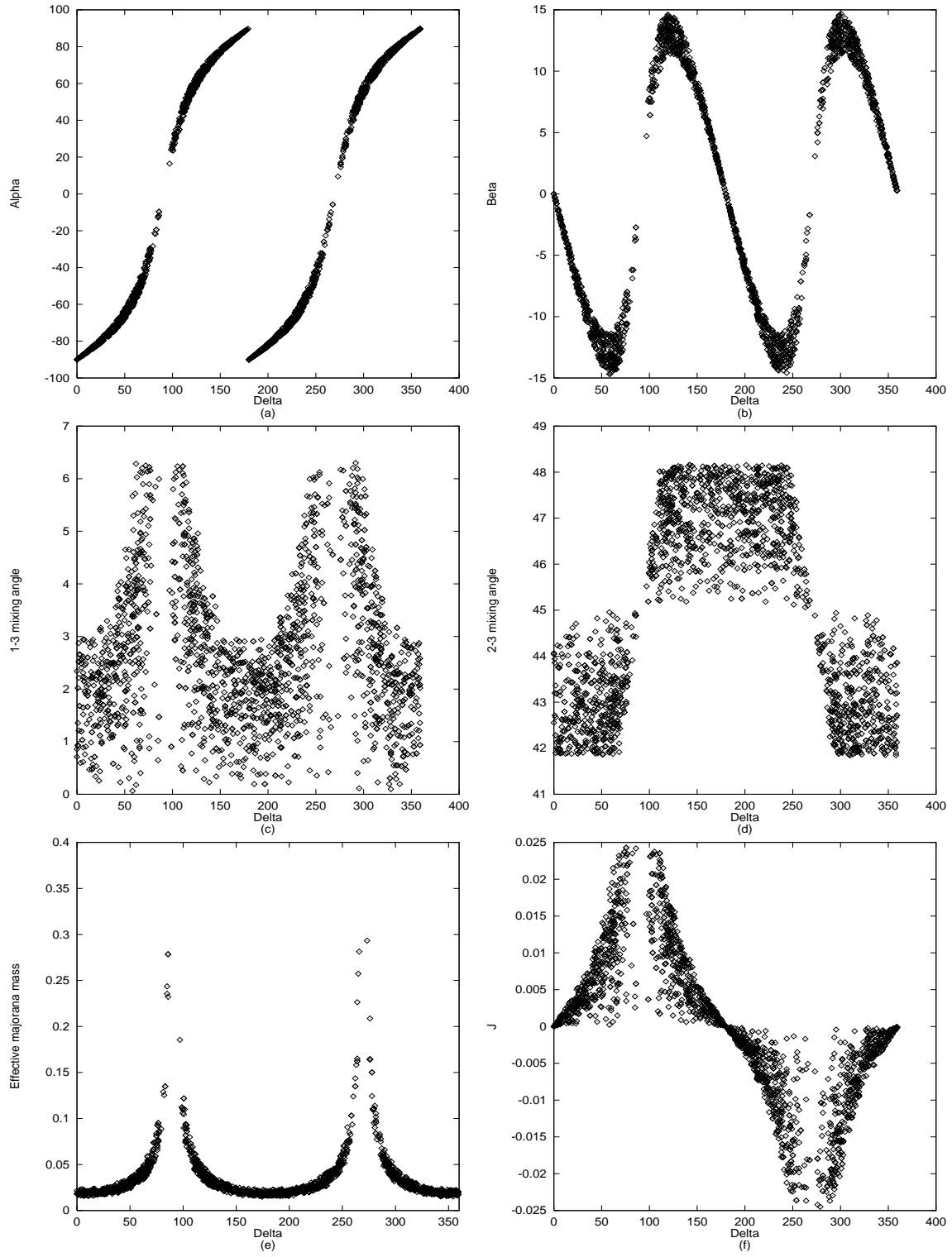


Figure 6: The correlation plots for CP-violating phase δ for neutrino mass matrices of type C with inverted hierarchy.

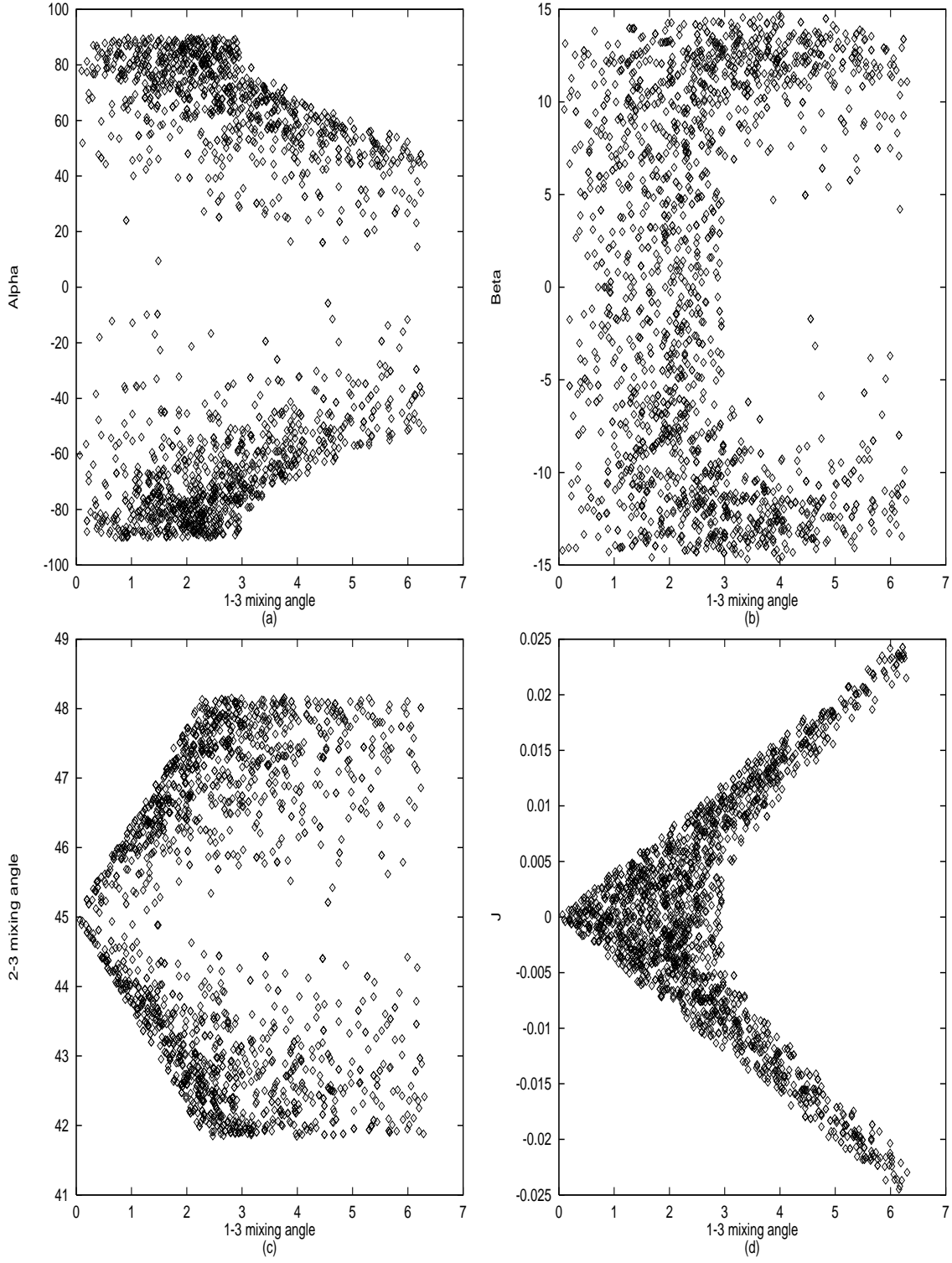


Figure 7: The correlation plots for the mixing angle θ_{13} for neutrino mass matrices of type C with inverted hierarchy.

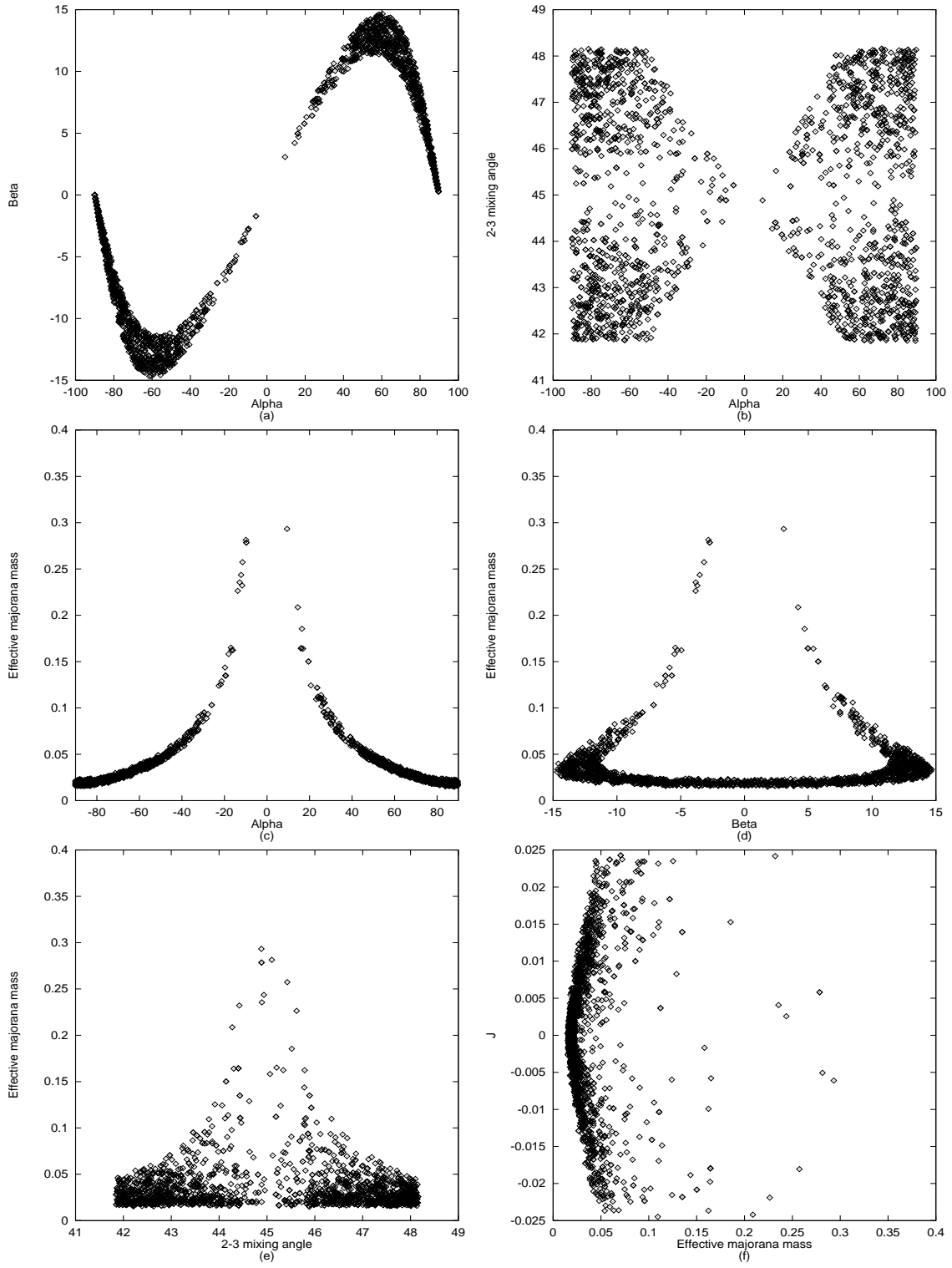


Figure 8: Some other important correlation plots for neutrino mass matrices of type C with inverted hierarchy.